

Dependence of atomic parity-violation effects on neutron skins and new physics

A. V. Viatkina¹, D. Antypas¹, M. G. Kozlov^{2,3}, D. Budker^{1,4}, V. V. Flambaum^{1,5}

¹*Helmholtz Institute, Johannes Gutenberg-Universität Mainz, 55099 Mainz, Germany*

²*Petersburg Nuclear Physics Institute of NRC "Kurchatov center", Gatchina, Leningrad District 188300, Russia*

³*St. Petersburg Electrotechnical University LETI, Prof. Popov Str. 5, 197376 St. Petersburg, Russia*

⁴*Department of Physics, University of California, Berkeley, California 94720-7300, USA*

⁵*School of Physics, University of New South Wales, Sydney 2052, Australia*

(Dated: March 4, 2019)

We estimate the relative contribution of nuclear structure and new physics couplings to the parity non-conserving spin-independent effects in atomic systems, for both single isotopes and isotopic ratios. General expressions are presented to assess the sensitivity of isotopic ratios to neutron skins and to couplings beyond standard model at tree level. The specific coefficients for these contributions are calculated assuming Fermi distribution for proton and neutron nuclear densities for isotopes of Cs, Ba, Sm, Dy, Yb, Pb, Fr, and Ra. The present work aims to provide a guide to the choice of the best isotopes and pairs of isotopes for conducting atomic PNC measurements.

I. INTRODUCTION

Parity-nonconserving (PNC) effects observed in low-energy atomic experiments can provide a precise test of the standard model (SM) and serve as probes of its possible extensions. For a range of new-physics scenarios, notably for those which manifest themselves at lower energies, atomic tests can give complementary and sometimes better probe compared to experiments at high-energy colliders [1]. Currently, a number of experiments are being conducted, with the aim to measure the PNC effects in isotopic chains, for example Yb experiment in Mainz [2] and Fr experiment at TRIUMF [3].

Parity violating weak interaction between electron and quarks in a nucleus is mediated by the heavy Z^0 -boson ($M_Z \approx 91.2$ GeV), therefore on atomic and even nuclear energy scales it can be considered point-like. This interaction is given by the product of axial and vector neutral currents. One can neglect internal nucleon structure and combine individual quarks into protons and neutrons [4], in which case the PNC part of the Hamiltonian for neutral currents is written as:

$$\begin{aligned} \hat{h}_{\text{PNC}} &= \hat{h}_{SI} + \hat{h}_{SD} \\ &= \frac{G_f}{\sqrt{2}} \sum_B [C_{1B} \bar{e} \gamma_\mu \gamma_5 e \bar{B} \gamma_\mu B + C_{2B} \bar{e} \gamma_\mu e \bar{B} \gamma_\mu \gamma_5 B], \end{aligned} \quad (1)$$

where the two terms represent the nuclear spin independent (SI) and dependent (SD) parts, respectively. The operators B and e are nucleon and electron field operators, B runs over all protons (p) and neutrons (n) in the nucleus, γ_μ ($\mu = 0, 1, 2, 3$) and γ_5 are Dirac matrices and

$$G_f \approx 1.16638 \times 10^{-5} (\hbar c)^3 \text{GeV}^{-2} \quad (2)$$

is the Fermi weak-interaction constant. With θ_W being the Weinberg angle ($\sin^2 \theta_W \approx 0.23$) and nucleon axial charge being $g_A \approx 1.26$, the coefficients from (1), calcu-

lated in the lowest tree-level approximation of SM, are

$$C_{1p} = \frac{1}{2}(1 - 4 \sin^2 \theta_W) \approx 0.04, \quad (3)$$

$$C_{1n} = -\frac{1}{2}, \quad (4)$$

$$C_{2p} = -C_{2n} = \frac{1}{2}(1 - 4 \sin^2 \theta_W) g_A \approx 0.05. \quad (5)$$

Spin-independent \hat{h}_{SI} arises from the coupling of electron axial current and nucleon vector current. On the other hand, \hat{h}_{SD} comes from the coupling of electron vector current and nucleon axial current. All nucleons contribute coherently to \hat{h}_{SI} , but protons considerably less than neutrons (since $C_{1p} \ll C_{1n}$). In SD part only the valence nucleon contributes, moreover, both C_{2p} and C_{2n} are small. The \hat{h}_{SD} contribution is thus typically three orders of magnitude smaller than that of \hat{h}_{SI} . It should be noted that there exist other spin-dependent PNC contributions, arising for example from nuclear anapole moment, but they are usually still small in comparison to the first term of (1) [5, 6].

In this work we focus on \hat{h}_{SI} . Treating nucleons non-relativistically, one can rewrite it as an effective single-electron operator

$$\hat{h}_{SI} = \frac{G_f}{\sqrt{2}} [C_{1p} Z \rho_p(r) + C_{1n} N \rho_n(r)] \gamma_5, \quad (6)$$

where ρ_p and ρ_n signify proton and neutron densities as functions of a radial variable r , both normalized to unity. Most often, the difference of ρ_p and ρ_n is neglected and (6) turns into

$$\hat{h}_{SI,0} = \frac{G_f}{2\sqrt{2}} Q_W \rho(r) \gamma_5, \quad (7)$$

$$Q_W \equiv 2C_{1p} Z + 2C_{1n} N, \quad (8)$$

$$\rho_p(r) = \rho_n(r) \equiv \rho(r). \quad (9)$$

Here Q_W is the weak charge of the nucleus. Within tree-level of SM, the weak charge is given by

$$Q_W = Z(1 - 4 \sin^2 \theta_W) - N. \quad (10)$$

The more precise SM value of Q_W with radiative corrections included, accurate at the 0.1% level, is [7]:

$$Q_W \approx -0.989N + 0.071Z . \quad (11)$$

The values of (10) and (11) differ typically by 0.5%, for the isotopes investigated in Section IV.¹

For the purposes of this work, it is necessary to account for the difference between proton ρ_p and neutron ρ_n nuclear densities. Let us return to the effective Hamiltonian (6). This operator enters PNC atomic observables through a matrix element between two atomic states with relativistic wave functions ψ_j and ψ_i :

$$\begin{aligned} \mathcal{M} &= \langle j | \hat{h}_{SI} | i \rangle \\ &= \frac{G_f}{2\sqrt{2}} \left[2C_{1p}Z \int \rho_p(r) \psi_j^\dagger \gamma_5 \psi_i d^3r \right. \\ &\quad \left. + 2C_{1n}N \int \rho_n(r) \psi_j^\dagger \gamma_5 \psi_i d^3r \right]. \end{aligned} \quad (12)$$

To simplify further calculations, we consider only the single-electron ψ of a valence electron. Due to the point-like nature of the weak interaction, the matrix element (12) is the largest between s and $p_{1/2}$ states. Using the Dirac wave functions for these orbitals inside a uniformly charged spherical nucleus and integrating over angles (see Appendix), one can show that

$$\int d\phi \int d\theta \psi_{p_{1/2}}^\dagger \gamma_5 \psi_s = \mathcal{A}_{ps} \mathcal{N} f_{ps}(r) , \quad (13)$$

and

$$\mathcal{M} = \frac{G_f}{2\sqrt{2}} \mathcal{A}_{ps} \mathcal{N} \tilde{Q}_{W,ps} , \quad (14)$$

where \mathcal{A}_{ps} is the atomic factor which has no dependence on nuclear parameters², \mathcal{N} is a normalization factor dependent on the nuclear charge radius, $f_{ps}(r)$ is the spatial variation of electron wave function density over the nucleus with $f_{ps}(0) = 1$, and $\tilde{Q}_{W,ps}$ is an effective nuclear weak charge, which quantifies the coupling strength between s and $p_{1/2}$ electrons. For simplicity, let us label $\tilde{Q}_{W,ps} \equiv \tilde{Q}$ and $f_{ps}(r') \equiv f(r')$. Within the limits of SM and at the tree-level approximation, one writes:

$$\tilde{Q} = Zq_p(1 - 4\sin^2\theta_W) - Nq_n, \quad (15)$$

$$q_p = \int \rho_p(r') f(r') dr', \quad (16)$$

$$q_n = \int \rho_n(r') f(r') dr'. \quad (17)$$

Here ρ_p and ρ_n are normalized to unity. Throughout the present work, we assume proton density equal to charge density $\rho_p = \rho_{\text{charge}}$.³

It is useful to introduce an equivalent radius R as a substitute for the rms radius $r_{\text{rms}} = \sqrt{\langle r^2 \rangle}$. In the case of a sharp-edge uniform spherical nucleus (SE model), from the definition of $\langle r^2 \rangle$, the two radii are related as:

$$r_{\text{rms}}^2 \equiv \langle r^2 \rangle = \frac{4\pi \int_0^R r'^2 \cdot r'^2 dr'}{4\pi \int_0^R r'^2 dr'} = \frac{3}{5} R^2 . \quad (18)$$

It should be noted that the expression of R through r_{rms} varies according to the nuclear density model used.

As follows from expressions for s and $p_{1/2}$ wave functions presented in Appendix, the normalization factor \mathcal{N} in (14) can be expressed through the proton distribution equivalent radius:

$$\mathcal{N} = \left(\frac{2ZR_p}{a_B} \right)^{2\gamma-2} . \quad (19)$$

Here a_B is Bohr radius and $\gamma = \sqrt{1 - (\alpha Z)^2}$, with α being fine structure constant and Z the atomic number.

Some classes of interactions beyond SM would contribute to the observed nuclear weak charge Q_W [9] and, correspondingly, to the effective nuclear weak charge \tilde{Q} :

$$\tilde{Q}_{\text{new}} = \tilde{Q} + \Delta\tilde{Q} . \quad (20)$$

An observation of $\Delta\tilde{Q}$ would be a hint for beyond SM interactions.

Uncertainties in the knowledge of the neutron distribution ρ_n , however, may hinder the extraction of $\Delta\tilde{Q}$ for neutron-rich nuclei. The problem in our case would be the poorly known radius of neutron distribution for most elements. The difference between radii of neutron and proton distributions is often referred to as *neutron skin*. For example, it was measured in ²⁰⁸Pb by PREX collaboration to be $0.33^{+0.16}_{-0.18}$ fm [10].

In [11], the PNC transition amplitude between the 6s and 7s states of neutral ¹³³Cs was measured with an accuracy of 0.35%. There is only one electron above closed shells in Cs, which makes precise atomic calculations feasible and the electronic part \mathcal{A}_{ps} can be accounted for by numerical calculations without acquiring significant errors [12–14]. Taking into account neutron-distribution corrections [15], Q_W of Cs was found to be in agreement with SM, leading to strong constraints on possible new-physics scenarios.

In heavy atoms, the PNC effect should be enhanced, since the atomic PNC observable related to (14) grows faster than Z^3 [16], but the interpretation of single-isotope measurement requires precise evaluation of \mathcal{A}_{ps} , which, for atoms with multiple valence electrons, is far

¹ Radiative corrections from Eq. (11) should be added to the final results for \tilde{Q} .

² In case one wants to account for it, a small nuclear-parameter-dependent contribution of an isotope shift to atomic wave functions should be included in the normalization factor \mathcal{N} .

³ A small difference is examined in [8].

from trivial. It was proposed [17] to measure ratios of PNC matrix elements in different isotopes of the same atom, thereby canceling out the atomic part:

$$\mathcal{R} = \frac{\mathcal{M}'}{\mathcal{M}} = \left(\frac{R'_p}{R_p}\right)^{2\gamma-2} \frac{\tilde{Q}'}{\tilde{Q}}. \quad (21)$$

Here \mathcal{M} and \mathcal{M}' correspond to the matrix elements (14) for isotopes of a given element with N and N' neutrons, respectively. Moreover, it was pointed out in [4, 18] that isotopic ratios are more sensitive to neutron-distribution uncertainties, compared to measurements in a single isotope. Isotopic ratios are less sensitive to certain types of new physics [9], on the other hand their reach is complementary to single-isotopes measurements. It is thus possible [4, 19] to use isotopic comparison to probe neutron skins, test various nuclear-structure models and search for new physics.

This work is organized as follows: in section II we derive analytical expressions for isotopic ratios (21) in sharp-edge and Fermi distribution models of the nuclear density, and investigate the contributions of neutron skin and new physics to these ratios. Section III is dedicated to a brief discussion of the role of nuclear deformations in spin-independent atomic PNC effects. In section IV we evaluate the coefficients of different contributions to the nuclear part $\mathcal{N}\tilde{Q}$ in (14) for a list of atoms of experimental interest for PNC measurements, namely Cs, Ba, Sm, Dy, Yb, Pb, Fr, and Ra. We discuss our results in the section V and present our conclusions in section VI.

II. ISOTOPIC RATIOS

Let us examine the sensitivity of isotopic ratios to new couplings manifested in the effective nuclear weak charge. Here we split the hypothetical new physics correction $\Delta\tilde{Q}$ to the effective weak charge (20) into proton and neutron

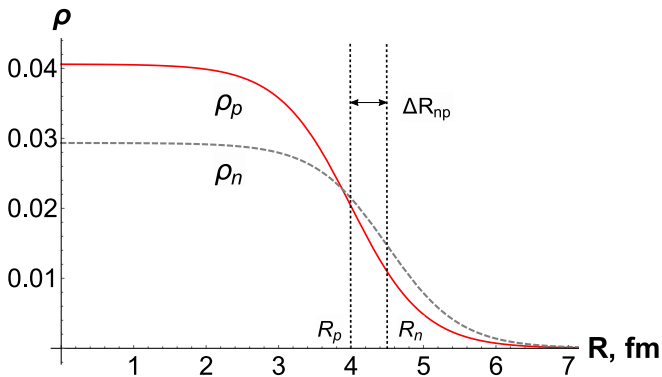


Figure 1: Normalized Fermi distribution of density of nucleons ρ , as defined in (30), for values of the diffuseness $z = 0.5$ fm. Here R_p and R_n are the equivalent radii of proton ρ_p and neutron ρ_n densities and ΔR_{np} is their difference.

contributions:

$$\Delta\tilde{Q} = Z\Delta\tilde{Q}^P + N\Delta\tilde{Q}^N. \quad (22)$$

For the present purposes, we can roughly assume $\tilde{Q} \approx -N$. To first order of Taylor expansion and denoting $\Delta N = N' - N$, one can write:

$$\frac{\tilde{Q}'}{\tilde{Q}} = \frac{-N' + \Delta\tilde{Q}'}{-N + \Delta\tilde{Q}} \approx \frac{N'}{N} \left[1 + \frac{Z\Delta N}{NN'} \Delta\tilde{Q}^P \right]. \quad (23)$$

Isotopic ratios are therefore primarily sensitive to the new proton couplings $\Delta\tilde{Q}^P$ (or, equivalently, twice as sensitive to the u -quark than to the d -quark couplings).

Now consider the nuclear-structure corrections [9, 18]. As a first approximation, we use a simplified model of the nucleus: proton and neutron densities are concentric sharp-edge spheres of given radii R_p and R_n . Using the expansions of Dirac wave functions of s and $p_{1/2}$ electrons inside the nucleus, one can show that the normalized wave-function density $f(r)$ inside the nucleus [see Eq. (13) and formulas in the Appendix] is:

$$f(r) = 1 - \frac{1}{2}(Z\alpha)^2 \left[\frac{r^2}{R_p^2} - \frac{1}{5} \frac{r^4}{R_p^4} + \frac{1}{75} \frac{r^6}{R_p^6} \right] + \dots \quad (24)$$

Performing the integrations in (16) and (17), one finds:

$$q_p = 1 - \frac{817}{3150}(Z\alpha)^2 + \mathcal{O}(Z\alpha)^4. \quad (25)$$

The function q_p is insensitive to the nuclear parameters R_p and R_n to first order in $(Z\alpha)^2$, and

$$q_n = 1 - (Z\alpha)^2 \left[\frac{3}{10} \frac{R_n^2}{R_p^2} - \frac{3}{70} \frac{R_n^4}{R_p^4} + \frac{1}{450} \frac{R_n^6}{R_p^6} \right] + \mathcal{O}(Z\alpha)^4. \quad (26)$$

In the sharp-edge spherical model, the radius of the sphere is expressed through the rms radius as [see (18)]

$$R^2 = \frac{5}{3} r_{\text{rms}}^2. \quad (27)$$

Let us define a neutron skin parameter using proton r_p and neutron r_n rms radii:

$$y \equiv \frac{r_n^2}{r_p^2} - 1 \quad (28)$$

and assume that it is small. We define the thickness of a neutron skin as the difference between neutron and proton rms radii: $\Delta r_{np} = r_n - r_p$, then $y \approx 2\Delta r_{np}/r_p$. To first order in y (28) the integral q_n simplifies to:

$$\begin{aligned} q_n &= 1 - (Z\alpha)^2 \left(\frac{817}{3150} + \frac{116}{525} y \right) + \mathcal{O}(Z\alpha)^4 \\ &= q_p - \frac{116}{525} (Z\alpha)^2 y + \mathcal{O}(Z\alpha)^4. \end{aligned} \quad (29)$$

Table I: Mean values of the coefficients $\bar{\varepsilon}$ from (33) and $\bar{\eta}$ from (34) for different elements, assuming Fermi distribution of nuclear density with the diffuseness value $z = 0.53(4)$ fm [20]. Here $\Delta\varepsilon$ and $\Delta\eta$ represent the maximum deviation of ε and η from the mean value in isotopes A of a given element. For comparison, in the sharp-edge model, $\varepsilon_0 \approx 0.2594$ and $\eta_0 \approx 0.2210$. Thus, generally, $\varepsilon > \varepsilon_0$ and $\eta > \eta_0$.

	Z	A	$\bar{\varepsilon}$	$\Delta\varepsilon$	$\bar{\eta}$	$\Delta\eta$
Cs	55	131 – 137	0.2974	0.0001	0.24487	0.00007
Ba	56	130 – 138	0.2970	0.0001	0.24460	0.00007
Sm	62	144 – 154	0.294	0.001	0.2427	0.0007
Dy	66	156 – 164	0.2913	0.0005	0.2412	0.0003
Yb	70	168 – 176	0.2900	0.0004	0.2404	0.0002
Pb	82	202 – 208	0.2877	0.0002	0.2390	0.0001
Fr	87	207 – 228	0.2859	0.0009	0.2379	0.0006
Ra	88	208 – 232	0.286	0.001	0.2378	0.0006

One can evaluate integrals q_p and q_n using a more realistic approach, with the neutron and proton nuclear density having the shape of Fermi distribution:

$$\rho_F(r, R_0) = \mathcal{B} \frac{1}{1 + \exp\left(\frac{r-R_0}{z}\right)}, \quad (30)$$

where \mathcal{B} is normalization constant such that

$$\int_0^\infty \rho_F(r, R_0) r^2 dr = 1, \quad (31)$$

where the parameter R_0 is the radius of the distribution and z the diffuseness (see Fig. 1). Here the rms radius is expressed through R_0 as:

$$r_{\text{rms}}^2 = \langle r^2 \rangle \approx \frac{3}{5} R_0^2 + \frac{7}{5} \pi^2 z^2. \quad (32)$$

In the limit of $z \rightarrow 0$ the $\rho_F(R, R_0)$ reduces to the sharp-edge spherical distribution with radius R_0 . For further calculations, we use the mean value of diffuseness of experimental charge distributions $z = 0.53(4)$ fm presented in Ref. [20]. Using the approach similar to that employed for obtaining Eqs. (25) and (29), one can show that to first order in $(Z\alpha)^2$, integrals (16) and (17) can be expressed as:

$$q_p = 1 - \varepsilon(Z\alpha)^2 + \mathcal{O}(Z\alpha)^4, \quad (33)$$

$$q_n = q_p - \eta y (Z\alpha)^2 + \mathcal{O}(Z\alpha)^4, \quad (34)$$

assuming $|y| \ll 1$. Here ε and η become functions of the nuclear radius R , but remain close to the sharp-edge values $\varepsilon_0 = 817/3150 \approx 0.2594$ and $\eta_0 = 116/525 \approx 0.2210$ (see Table I). In fact, the dependence of ε and η on R is weak and they can be treated as constants for a selected element. A more detailed approach to analytic calculation of the dependence of a PNC matrix element on the nuclear shape was described in [21].

Let us estimate the influence of nuclear parameters R_p and R_n on the isotopic ratio. For this analysis we assume

no new physics couplings ($\Delta\tilde{Q} = 0$). With $(1 - 4 \sin^2 \theta) \equiv \xi$ the ratio (21) reads:

$$\begin{aligned} \mathcal{R} &= \left(\frac{R'_p}{R_p}\right)^{2\gamma-2} \frac{Z\xi q'_p - N'q'_n}{Z\xi q_p - Nq_n} \\ &= \left(\frac{R'_p}{R_p}\right)^{2\gamma-2} \frac{N'}{N} \varkappa. \end{aligned} \quad (35)$$

Here we retained only the first order in the expansion of \mathcal{R} in $(Z\alpha)^2$ and introduced the notations: $\Delta N = N' - N$ and \varkappa :

$$\varkappa \equiv \frac{q'_p}{q_p} \left[1 + \frac{Z\xi\Delta N}{NN'} - (Z\alpha)^2 \left(\frac{\eta'y'}{q'_p} - \frac{\eta y}{q_p} \right) \right]. \quad (36)$$

If one assumes the sharp-edge model where $q'_p = q_p = q_{p,0}$ and $\eta' = \eta = \eta_0$, then \varkappa simplifies to:

$$\varkappa_0 = 1 + \frac{Z\xi\Delta N}{NN'} - \frac{\eta_0}{q_{p,0}} (Z\alpha)^2 (y' - y). \quad (37)$$

Here the second term comes from the proton contribution to the nuclear effective weak charge and it does not depend on the nuclear structure. The third term gives the explicit dependence of κ_0 on the change of the ratio of neutron and proton radii; in the sharp-edge model, if the neutron radius is strictly proportional to proton radius, $y' - y$ sums to zero.

Let us write an expansion of the isotopic ratio (21), which combines both new physics (23) and neutron skin (36) contributions, in order to examine their joined contributions to the ratio ($N' > N$):

$$\begin{aligned} \mathcal{R} &\approx \left(\frac{R'_p}{R_p}\right)^{2\gamma-2} \frac{\tilde{Q}'}{\tilde{Q}} = \left(\frac{R'_p}{R_p}\right)^{2\gamma-2} \frac{N'}{N} \frac{q'_p}{q_p} \times \\ &\left[1 + \frac{Z\xi\Delta N}{NN'} - (Z\alpha)^2 \left(\frac{\eta'y'}{q'_p} - \frac{\eta y}{q_p} \right) + \right. \\ &\left. \Delta\tilde{Q}^N \frac{q'_p - q_p}{q'_p q_p} + Z\Delta\tilde{Q}^P \frac{N'q'_p - Nq_p}{N'Nq'_p q_p} \right]. \end{aligned} \quad (38)$$

In the sharp-edge model:

$$\begin{aligned} \mathcal{R} &\approx \left(\frac{R'_p}{R_p}\right)^{2\gamma-2} \frac{N'}{N} \times \\ &\left[1 + \frac{Z\Delta N}{NN'} \left(\xi + \frac{\Delta\tilde{Q}^P}{q_{p,0}} \right) - \frac{\eta_0}{q_{p,0}} (Z\alpha)^2 (y' - y) \right]. \end{aligned} \quad (39)$$

As Table I indicates, ε and η are almost constant for a given element, and therefore the values of q_p , q'_p and η , η' are close. The expressions (37) and (39), initially derived for sharp-edge model, can thus also be used within the Fermi distribution model, provided that $q_{p,0}$ is replaced with \bar{q}_p and η_0 with $\bar{\eta}$ (see Table I). The Eq. (39) then becomes

$$\begin{aligned} \mathcal{R} &\approx \left(\frac{R'_p}{R_p}\right)^{2\gamma-2} \frac{N'}{N} \times \\ &\left[1 + \frac{Z\Delta N}{NN'} \left(\xi + \frac{\Delta\tilde{Q}^P}{\bar{q}_p} \right) - \frac{\bar{\eta}}{\bar{q}_p} (Z\alpha)^2 (y' - y) \right]. \end{aligned} \quad (40)$$

Note that $\Delta\tilde{Q}^P$ enters the isotopic ratio (40) the same way as ξ . New physics corrections to proton coupling would thus manifest themselves similarly to corrections to Weinberg angle. In fact, probing the Weinberg angle in low-energy experiments presents a unique opportunity for search for a number of new physics scenarios, such as dark Z boson [1, 22].

The characteristic scales of $\Delta\tilde{Q}^P$ for various new physics scenarios were discussed e.g. in [9]; for a more recent review see [1]. Constraints on ΔQ^P arising in presence of additional Z' bosons, were recently reported in [2], and were based on measurements of Yb PNC amplitudes and atomic calculations [23].

III. NUCLEAR DEFORMATION

As Eq. (40) shows, the value of the ratio \mathcal{R} depends primarily on the neutron numbers and radii of the involved isotopes. It is thus most efficient to make use of a pair of isotopes with the largest possible ΔN to maximize the ratio.

A large change in rms radius between two isotopes can occur when there is a significant change in nuclear deformation. The simplest case of quadrupole deformation of a sharp-edge nucleus is a surface:

$$r = r_0 (1 + \beta Y_2^0) , \quad (41)$$

where r_0 is a radius parameter and Y_2^0 a spherical harmonic

$$Y_2^0 = \sqrt{\frac{5}{16\pi}} (3 \cos^2 \theta - 1) . \quad (42)$$

Here β is the deformation parameter; usually, $\beta \lesssim 1/3$ [24]. The mean charge radius that corresponds to the surface (41) would be expressed as:

$$\langle r^2 \rangle_\beta = \frac{3}{5} r_0^2 \left(1 + \frac{7}{4\pi} \beta^2 \right) . \quad (43)$$

Given the constant volume of the nucleus, the mean charge radii of the deformed $\langle r^2 \rangle_\beta$ and of the initial spherical nucleus $\langle r^2 \rangle_0$ are related through:

$$\langle r^2 \rangle_\beta = \langle r^2 \rangle_0 \left(1 + \frac{5}{4\pi} \beta^2 \right) . \quad (44)$$

The quadrupole deformation is directly connected to the nuclear intrinsic quadrupole moment Q [25]:

$$Q = \frac{3}{\sqrt{5\pi}} Z r_0^2 \beta (1 + 0.36\beta) . \quad (45)$$

There could be a weak quadrupole moment as well, due to the deviation of neutron distribution from the spherical shape. It would result in a tensor PNC interaction between the nucleus and the electrons, as discussed in

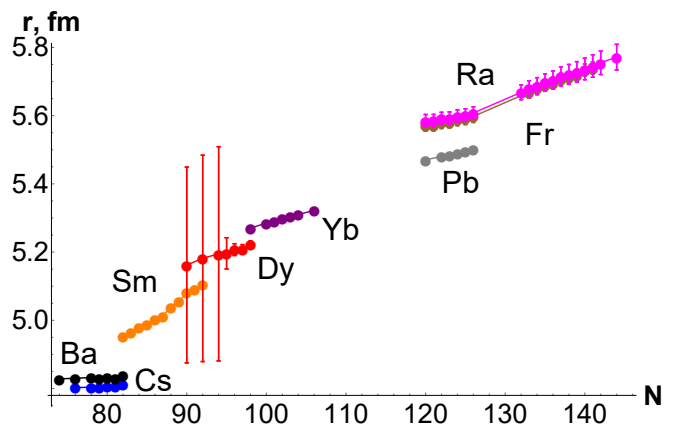


Figure 2: Experimental rms proton radii (r) for eight elements, as listed in [28] and Table II, plotted against the neutron numbers (N) of each element. On the scale of this plot, uncertainties are visible only for Dy and Ra. The points for Ra and Fr almost completely overlap. The first isotopes in the lists of elements are: ^{131}Cs , ^{130}Ba , ^{144}Sm , ^{156}Dy , ^{168}Yb , ^{202}Pb , ^{207}Ra and ^{208}Fr . It appears that the uncertainties listed in [28] may be overestimated and there may be correlations in the radii of different isotopes of a given element.

Refs. [26, 27]. A tensor interaction has different selection rules from a scalar (spin-independent) interaction, so it is possible to separate one from another in an experiment. Therefore, for the purposes of the present work, it is sufficient to treat deformed nuclei as spherical nuclei with equivalent charge radius R_p^2 .

IV. EVALUATION OF PARAMETERS IN PNC MATRIX ELEMENT FOR SPECIFIC ISOTOPES

Let us find the dependence of the nuclear part in (14) on the ratio of the neutron and proton equivalent radii R_n^2/R_p^2 and on the new-physics couplings to protons and neutrons in isotopes proposed for PNC experiments [1]. The neutron-skin parameter y is defined in Eq. (28). To first order in $(Z\alpha)^2$ and y , the nuclear part of (14) can be expressed as:

$$\begin{aligned} \mathcal{N}\tilde{Q} &= \left(\frac{2ZR_p}{a_B} \right)^{2\gamma-2} \left[Zq_p(1 - 4\sin^2\theta) - Nq_p \right. \\ &\quad \left. + \eta N(Z\alpha)^2 y + Z\Delta\tilde{Q}^P + N\Delta\tilde{Q}^N \right] \\ &\equiv \left(\frac{2ZR_p}{a_B} \right)^{2\gamma-2} \left[B_0 + B_1 y + Z\Delta\tilde{Q}^P + N\Delta\tilde{Q}^N \right] , \end{aligned} \quad (46)$$

defining

$$B_0 = [Z(1 - 4\sin^2\theta) - N] q_p , \quad (47)$$

$$B_1 = \eta N(Z\alpha)^2 . \quad (48)$$

For our calculations, we use the Fermi distribution of nucleons. We substitute the corresponding values of N , Z , r_p and $z = 0.53(4)$ fm for isotopes of Cs, Ba, Sm, Dy, Yb, Pb, Fr and Ra into Eq. (46), compute the coefficients B_0 and B_1 and list the results in Table II. The rms nuclear charge radii r_p are taken from Ref. [28]. The errors presented in Table II come from the predominantly experimental errors in r_p and the error in the value of z . If one used SE model in contrast to the Fermi distribution described above, the normalization $\mathcal{N} = (2ZR_p/a_B)^{2\gamma-2}$ would be lower by 2-3%, the values of q_p and B_0 would change by approximately 1%, whereas the coefficient B_1 would decrease by 7 – 10%.

Let us examine the role of experimental uncertainties in nuclear charge radius in a possible extraction of neutron-skin thickness. Based on neutron-skin calculations [29], a typical value of the parameter y for the isotopes considered in the present work would be 0.04–0.09. If one assumes that both the nuclear part of the PNC amplitude $\mathcal{N}\tilde{Q}$ and the weak charge Q_W are known with a 0.1% certainty, whereas the experimental uncertainties of charge radii are as listed in [28] and $z = 0.53(4)$, then the error in y is $\Delta y \approx 0.03 - 0.05$, with the tendency of Δy to decrease with Z . This error is typically more than 50% of the value of y , notably for lighter atoms. If the uncertainty of $\mathcal{N}\tilde{Q}$ is raised to 0.3%, the error in y becomes more than its value in lighter atoms and more than a half of its value in heavy atoms. It is thus crucial for the extraction of y from a single-isotope amplitude $\mathcal{N}\tilde{Q}$ to know with high accuracy both the charge radius and the diffuseness of the nuclei. Indeed, a large portion of the resulting error comes from the uncertainty in z . If one sets $\Delta z = 0$ (given the case of 0.1% certainty for $\mathcal{N}\tilde{Q}$ and Q_W), the reduction in Δy is 30 – 50%. Interpreting experimental results thus poses a challenge for nuclear models.

V. ANALYSIS AND OUTLOOK

A. Single isotope

It is convenient to express the size of nuclear-structure corrections as a fraction of the dominant PNC effect arising solely from $\hat{h}_{SI,0}$ [Eq. (7)]:

$$\mathcal{M}_0 = \langle j | \hat{h}_{SI,0} | i \rangle = \frac{G_f}{2\sqrt{2}} (2C_{1p}Z + 2C_{1n}N) I_p, \quad (49)$$

$$\mathcal{M}_1 = \langle j | \hat{h}_{SI} | i \rangle = \frac{G_f}{2\sqrt{2}} (2C_{1p}Z I_p + 2C_{1n}N I_n), \quad (50)$$

$$I_p = \int \rho_p(r) \psi_j^\dagger \gamma_5 \psi_i d^3r, \quad (51)$$

$$I_n = \int \rho_n(r) \psi_j^\dagger \gamma_5 \psi_i d^3r, \quad (52)$$

thus leading to

$$\frac{\delta E_{\text{PNC}}^{\text{n.s.}}}{E_{\text{PNC}}} = \frac{\mathcal{M}_1 - \mathcal{M}_0}{\mathcal{M}_0} = \frac{2C_{1n}N}{Q_W} \left(\frac{I_n}{I_p} - 1 \right), \quad (53)$$

where Q_W is the SM nuclear weak charge defined in Eq. (8). Assuming, as most realistic nuclear models imply, that the distributions of protons and neutrons are not radically different in shape, we express first-order values of q_p and q_n in the form of (33) and (34). At the tree level and using the electron wave functions given in the Appendix, we obtain

$$\begin{aligned} \frac{\delta E_{\text{PNC}}^{\text{n.s.}}}{E_{\text{PNC}}} &= \frac{-N}{Q_W} \left(\frac{q_n}{q_p} - 1 \right) = \frac{N\eta y}{Q_W q_p} (Z\alpha)^2 \\ &= \frac{B_1}{Q_W q_p} y \equiv K y. \end{aligned} \quad (54)$$

Since $2K/(Z\alpha)^2 \approx 3/7$, the quantity (54) is approximately equal to that given by the commonly used formula (see e.g. [29]):

$$\frac{\delta E_{\text{PNC}}^{\text{n.s.}}}{E_{\text{PNC}}} = -\frac{3}{7} (Z\alpha)^2 \frac{\Delta R_{np}}{R_p}, \quad (55)$$

which comes from a more crude estimate of integrals q_p (16) and q_n (17) in the sharp-edge model. Eq. (55) slightly underestimates the effect of a neutron skin on the PNC amplitude E_{PNC} .

We estimate the ratio $\delta E_{\text{PNC}}^{\text{n.s.}}/E_{\text{PNC}}$ according to Eq. (53), using neutron skin thicknesses calculated in [29] and tree-level Q_W (10), taking into account uncertainties of r_0 and z . The results are presented in third-to-last column of Table II. The values of $\delta E_{\text{PNC}}^{\text{n.s.}}/E_{\text{PNC}}$ calculated with the simplified formula (54) would differ only insignificantly.

B. Isotopic ratio

From Eqs. (38) and (39) one can see that isotopic ratios are, indeed, largely insensitive to the new couplings to neutron $\Delta\tilde{Q}^N$. This allows one to isolate new proton couplings when taking a ratio of PNC effects in different isotopes.

The relative sensitivity to nuclear structure and new proton couplings in isotopic ratios is most obvious if we turn to the formula (40) and compare the coefficients

$$c_p \equiv \frac{Z\Delta N}{NN'}, \quad (56)$$

$$c_n \equiv -\frac{\tilde{\eta}}{q_p} (Z\alpha)^2. \quad (57)$$

Both coefficients (56) and (57) are, generally, of the order of 0.01. In lighter atoms, such as Cs and Ba, c_p can be greater than c_n , which implies slightly better sensitivity to new proton couplings, but in heavier atoms (Dy, Yb, Pb, Fr and Ra) c_n dominates.

To give an estimate for the relative size of proton and neutron contribution in the isotopic ratio, we substitute $(y' - y)$ based on the neutron skin calculations [29] and compare second and third terms in parentheses

in Eq. (40). The ratio of neutron to proton contribution to (40) is

$$\chi = \frac{c_n(y' - y)}{c_p \xi} \quad (58)$$

is ≈ 0.2 for all isotopes of Cs and Ba, ≈ 0.3 for Sm and Dy and varies between 0.3 and 0.6 for selected pairs of isotopes in Yb, Fr and Ra. The neutron distribution effect is thus more pronounced in heavier atoms. If one aims to avoid significant neutron skin contributions, it is better to choose lighter elements.

Since the equation (40) provides a good approximation for the Fermi model and the neutron-skin correction to the ratio depends solely on

$$y' - y = \left(\frac{R'_n}{R'_p} \right)^2 - \left(\frac{R_n}{R_p} \right)^2, \quad (59)$$

it means that the errors in neutron skins for different isotopes, if correlated, cancel out when an isotopic ratio is evaluated. The errors in y are indeed shown to be

correlated in Ref. [29]. This cancellation enables use of isotopic ratio measurements to search for new physics couplings.

If the aim is to detect the neutron skin effect in an isotopic ratio, it is meaningful to choose pairs of isotopes with greater relative neutron skin contribution:

$$\frac{\Delta_{n.s.}}{\mathcal{R}} = \frac{c_n(y' - y)}{1 + c_p \xi + c_n(y' - y)}. \quad (60)$$

Values of the above ratio for selected pairs of isotopes are presented in Table II.

A 0.1% uncertainty of nuclear weak charge Q_W would result in approximately 0.14% uncertainty of the ratio \mathcal{R} for any pair of isotopes considered, which is larger than or comparable to the neutron skin effect (60) in some of the pairs, but is about a half of $\Delta_{n.s.}/\mathcal{R}$ in others, prominently in heavier elements.

Note that the parameter c_n [Eq. (57)] is close in value to the sensitivity to neutron skin K [Eq. (54)] of an individual isotope, as indeed follows from their definition. Therefore in Table II we present only c_p and c_n .

Table II: Evaluated coefficients from Eqs. (46)–(48) for the nuclear factor of the PNC amplitude, expanded in Eq. (46). The parameter Z is the atomic number of an element, A is the atomic mass number, N the number of neutrons and r_p is the rms radius of a given isotope in fm [28]. The normalization constant is $\mathcal{N} = (2ZR_p/a_B)^{2\gamma-2}$, where R_p is the equivalent proton radius. The coefficients B_0 and B_1 are defined in Eqs. (47) and (48). The isotopic-ratio parameters c_p and c_n follow Eqs. (56) and (57). The initial reference isotope for c_p is always the first in the list belonging to each element, and c_n is the same for any pair of isotopes of a given element. Calculated differences between neutron and proton rms radii Δr_{np} come from Ref. [29]. Approximate values of neutron-skin contributions to single-isotope PNC amplitudes $\delta E^{n.s.}/E$ [Eq. (54)] and to the ratios of PNC amplitudes $\Delta_{n.s.}/\mathcal{R}$ [Eq. (60)] are listed in the third-to-last and second-to-last columns. The last column indicates ratios of neutron skin contributions to proton contributions χ in an isotopic ratio, defined in (58), for a given pair of isotopes. The reference isotope of an element for $\Delta_{n.s.}/\mathcal{R}$ and χ is always the first isotope with known Δr_{np} . Stable isotopes and isotopes with half-life longer than 10^8 s are written in boldface.

Element	A	N	r_p , fm	\mathcal{N}	q_p	B_0	B_1	c_p	c_n	Δr_{np} , fm	$\delta E^{n.s.}/E$	$\Delta_{n.s.}/\mathcal{R}$	χ
Cs	131	76	4.803(5)	2.111(5)	0.952(1)	-68.17(7)	3.00(5)	-	-0.04	0.139(34)	-0.0026(6)	-	-
$Z = 55$	133	78	4.804(5)	2.111(5)	0.952(1)	-70.07(8)	3.08(5)	0.02		0.158(37)	-0.0029(7)	-0.0003	0.2
	134	79	4.803(5)	2.111(5)	0.952(1)	-71.03(8)	3.12(5)	0.03					
	135	80	4.807(5)	2.111(5)	0.952(1)	-71.98(8)	3.16(5)	0.04		0.176(40)	-0.0032(7)	-0.0007	0.2
	136	81	4.806(5)	2.111(5)	0.952(1)	-72.93(8)	3.20(5)	0.04					
	137	82	4.813(5)	2.110(5)	0.952(1)	-73.88(8)	3.23(5)	0.05		0.193(42)	-0.0035(8)	-0.0010	0.2
Ba	130	74	4.828(5)	2.163(6)	0.950(1)	-66.07(7)	3.02(5)	-	-0.04	0.104(29)	-0.0020(6)	-	-
$Z = 56$	132	76	4.830(5)	2.163(6)	0.950(1)	-67.97(8)	3.10(5)	0.02		0.124(32)	-0.0024(6)	-0.0004	0.2
	133	77	4.829(5)	2.163(6)	0.950(1)	-68.92(8)	3.15(5)	0.03					
	134	78	4.832(5)	2.163(6)	0.950(1)	-69.87(8)	3.19(5)	0.04		0.143(34)	-0.0027(6)	-0.0007	0.2
	135	79	4.829(5)	2.163(6)	0.950(1)	-70.82(8)	3.23(5)	0.05					
	136	80	4.833(5)	2.163(6)	0.950(1)	-71.78(8)	3.27(5)	0.06		0.161(37)	-0.0030(7)	-0.0010	0.2
	137	81	4.831(5)	2.163(6)	0.950(1)	-72.73(8)	3.31(5)	0.07					
	138	82	4.838(5)	2.162(6)	0.950(1)	-73.68(8)	3.35(5)	0.07		0.179(40)	-0.0034(8)	-0.0014	0.2
Sm	144	82	4.952(3)	2.529(8)	0.940(1)	-72.39(9)	4.09(6)	-	-0.05	0.098(27)	-0.0022(6)	-	-
$Z = 62$	145	83	4.965(3)	2.527(8)	0.940(1)	-73.3(1)	4.13(6)	0.01					
	146	84	4.981(4)	2.525(8)	0.940(1)	-74.3(1)	4.18(6)	0.02		0.122(32)	-0.0028(7)	-0.0005	0.4
	147	85	4.989(4)	2.524(8)	0.940(1)	-75.2(1)	4.23(6)	0.03					
	148	86	5.004(3)	2.522(8)	0.940(1)	-76.2(1)	4.28(6)	0.04		0.144(35)	-0.0032(8)	-0.0010	0.3
	149	87	5.013(4)	2.521(8)	0.940(1)	-77.1(1)	4.32(6)	0.04					
	150	88	5.039(5)	2.518(7)	0.940(1)	-78.0(1)	4.37(6)	0.05		0.166(39)	-0.0037(9)	-0.0014	0.3
	151	89	5.055(6)	2.516(7)	0.940(1)	-79.0(1)	4.42(6)	0.06					
	152	90	5.082(6)	2.512(7)	0.940(1)	-79.9(1)	4.46(6)	0.07		0.187(43)	-0.004(1)	-0.0018	0.3

	153	91	5.093(7)	2.511(7)	0.940(1)	-80.9(1)	4.51(6)	0.07					
	154	92	5.105(7)	2.509(7)	0.940(1)	-81.8(1)	4.56(6)	0.08		0.219(48)	-0.005(1)	-0.0025	0.4
Dy	156	90	5.2(3)	2.81(5)	0.932(2)	-79.0(1)	5.04(9)	-	-0.06	0.135(35)	-0.0033(9)	-	-
Z = 66	158	92	5.2(3)	2.80(5)	0.932(2)	-80.9(1)	5.15(9)	0.02		0.150(37)	-0.004(1)	-0.0003	0.3
	160	94	5.2(3)	2.80(5)	0.932(2)	-82.7(1)	5.26(9)	0.03		0.164(38)	-0.004(1)	-0.0007	0.3
	161	95	5.20(5)	2.80(1)	0.932(1)	-83.7(1)	5.31(7)	0.04					
	162	96	5.21(2)	2.801(9)	0.932(1)	-84.6(1)	5.37(7)	0.05		0.178(40)	-0.004(1)	-0.0010	0.3
	163	97	5.21(1)	2.800(9)	0.932(1)	-85.5(1)	5.42(7)	0.05					
	164	98	5.22(1)	2.799(9)	0.933(1)	-86.5(1)	5.48(7)	0.06		0.191(42)	-0.005(1)	-0.0013	0.3
Yb	168	98	5.270(6)	3.15(1)	0.924(1)	-85.4(1)	6.15(8)	-	-0.07	0.141(35)	-0.004(1)	-	-
Z = 70	170	100	5.285(6)	3.15(1)	0.924(1)	-87.3(1)	6.27(8)	0.01		0.153(38)	-0.004(1)	-0.0003	0.3
	171	101	5.291(6)	3.15(1)	0.924(1)	-88.2(1)	6.34(8)	0.02					
	172	102	5.300(6)	3.15(1)	0.924(1)	-89.1(1)	6.40(8)	0.03		0.174(40)	-0.005(1)	-0.0008	0.4
	173	103	5.305(6)	3.15(1)	0.924(1)	-90.0(1)	6.46(8)	0.03					
	174	104	5.311(6)	3.15(1)	0.924(1)	-91.0(1)	6.52(8)	0.04		0.202(51)	-0.005(1)	-0.0016	0.5
	176	106	5.322(6)	3.14(1)	0.924(1)	-92.8(1)	6.64(9)	0.05		0.215(67)	-0.006(2)	-0.0019	0.4
Pb	202	120	5.471(2)	4.70(2)	0.897(2)	-101.7(2)	10.3(1)	-	-0.10				
Z = 82	204	122	5.480(1)	4.69(2)	0.897(2)	-103.5(2)	10.4(1)	0.01		0.172(44)	-0.006(2)	-	-
	205	123	5.483(2)	4.69(2)	0.897(2)	-104.4(2)	10.5(1)	0.02					
	206	124	5.490(1)	4.69(2)	0.897(2)	-105.3(2)	10.6(1)	0.02		0.184(46)	-0.007(2)	-0.0004	0.5
	207	125	5.494(1)	4.69(2)	0.897(2)	-106.2(2)	10.7(1)	0.03					
	208	126	5.501(1)	4.69(2)	0.897(2)	-107.1(2)	10.8(1)	0.03		0.200(50)	-0.007(2)	-0.0010	0.6
Fr	207	120	5.57(2)	5.66(3)	0.884(2)	-100.0(2)	11.5(1)	-	-0.11				
Z = 87	208	121	5.57(2)	5.66(3)	0.884(2)	-100.9(2)	11.6(1)	0.01					
	209	122	5.58(2)	5.65(3)	0.884(2)	-101.7(2)	11.7(1)	0.01		0.121(36)	-0.005(1)	-	-
	210	123	5.58(2)	5.65(3)	0.884(2)	-102.6(2)	11.8(1)	0.02					
	211	124	5.59(2)	5.65(3)	0.884(2)	-103.5(2)	11.9(1)	0.02		0.132(38)	-0.005(2)	-0.0004	0.5
	212	125	5.59(2)	5.65(3)	0.885(2)	-104.4(2)	12.0(1)	0.03					
	213	126	5.60(2)	5.64(3)	0.885(2)	-105.3(2)	12.1(1)	0.03		0.146(42)	-0.006(2)	-0.0010	0.5
	220	133	5.67(2)	5.61(3)	0.885(2)	-111.5(2)	12.7(1)	0.07					
	221	134	5.68(2)	5.60(3)	0.885(2)	-112.4(2)	12.8(1)	0.08		0.206(53)	-0.008(2)	-0.0032	0.6
	222	135	5.69(2)	5.60(3)	0.885(2)	-113.3(2)	12.9(1)	0.08					
	223	136	5.70(2)	5.59(3)	0.885(2)	-114.2(2)	13.0(1)	0.09					
	224	137	5.71(2)	5.59(3)	0.885(2)	-115.1(2)	13.1(1)	0.09					
	225	138	5.71(2)	5.59(3)	0.885(2)	-116.0(2)	13.2(1)	0.09					
	226	139	5.72(2)	5.58(3)	0.885(2)	-116.9(2)	13.3(1)	0.10					
	227	140	5.73(2)	5.58(3)	0.885(2)	-117.8(2)	13.4(1)	0.10					
	228	141	5.74(2)	5.57(3)	0.885(2)	-118.6(2)	13.5(1)	0.11					
Ra	208	120	5.59(2)	5.89(3)	0.882(2)	-99.6(2)	11.8(1)	-	-0.11				
Z = 88	209	121	5.59(2)	5.89(3)	0.882(2)	-100.5(2)	11.9(1)	0.01					
	210	122	5.59(2)	5.88(3)	0.882(2)	-101.4(2)	12.0(1)	0.01		0.111(34)	-0.005(1)	-	-
	211	123	5.59(2)	5.88(3)	0.882(2)	-102.3(2)	12.1(1)	0.02					
	212	124	5.60(2)	5.88(3)	0.882(2)	-103.1(2)	12.2(1)	0.02		0.123(37)	-0.005(2)	-0.0005	0.5
	213	125	5.60(2)	5.88(3)	0.882(2)	-104.0(2)	12.3(1)	0.03					
	214	126	5.61(2)	5.87(3)	0.882(2)	-104.9(2)	12.4(1)	0.03		0.136(40)	-0.006(2)	-0.0010	0.5
	220	132	5.67(2)	5.84(3)	0.882(2)	-110.2(2)	12.9(1)	0.07		0.181(49)	-0.008(2)	-0.0028	0.6
	221	133	5.68(2)	5.83(3)	0.882(2)	-111.1(2)	13.0(1)	0.07					
	222	134	5.69(2)	5.83(3)	0.882(2)	-112.0(2)	13.1(1)	0.08		0.195(52)	-0.008(2)	-0.0033	0.6
	223	135	5.70(3)	5.82(3)	0.882(2)	-112.9(2)	13.2(1)	0.08					
	224	136	5.70(3)	5.82(3)	0.882(2)	-113.8(2)	13.3(1)	0.09					
	225	137	5.72(3)	5.82(3)	0.882(2)	-114.7(2)	13.4(1)	0.09					
	226	138	5.72(3)	5.81(3)	0.882(2)	-115.6(2)	13.5(1)	0.10					
	227	139	5.73(3)	5.81(3)	0.882(2)	-116.4(2)	13.6(2)	0.10					
	228	140	5.74(3)	5.80(3)	0.882(2)	-117.3(2)	13.7(2)	0.10					
	229	141	5.75(3)	5.80(3)	0.882(2)	-118.2(2)	13.8(2)	0.11					
	230	142	5.76(3)	5.79(3)	0.883(2)	-119.1(2)	13.9(2)	0.11					
	232	144	5.77(4)	5.78(3)	0.883(2)	-120.9(2)	14.1(2)	0.12					

In Ref. [2] the PNC effects were measured in four even isotopes of Yb. Table III details the size of the neutron-skin contribution to the PNC amplitude in individual Yb isotopes and their ratios, according to neutron skin

values from [29] and Eqs. (54) and (60). The listed values indicate that it may be possible to detect the neutron skin contribution in an isotopic ratio of Yb if 0.1% level of accuracy is reached.

Table III: Relative contribution of the neutron-skin effect to the total PNC amplitude or a ratio of PNC amplitudes in Yb isotopes used in experiment [2], evaluated according to Eqs. (53), (58) and (60). We compute the difference between neutron and proton rms radii Δr_{np} from [29] and nuclear charge radii r_p from [28]. The ratio χ of neutron skin contribution to proton contribution in an isotopic ratio \mathcal{R} is defined in Eq. (58).

Z	A	r_p , fm	Δr_{np} , fm	$\frac{\delta E_{\text{PNC}}^{n.s.}}{E_{\text{PNC}}}$	$\Delta_{n.s.}/\mathcal{R}$	χ	
Yb	70	170	5.285(6)	0.153(38)	-0.004(1)	-	
		172	5.300(6)	0.174(40)	-0.005(1)	-0.0005	0.5
		174	5.311(6)	0.202(51)	-0.005(1)	-0.0013	0.6
		176	5.322(6)	0.215(67)	-0.006(2)	-0.0016	0.5

In order to obtain useful experimental information regarding the new physics couplings or the behavior of neutron skins, one would typically need to know the ratio \mathcal{R} with $\sim 0.1\%$ accuracy. Pairs of isotopes with large ΔN , e.g. ^{209}Fr and ^{221}Fr or ^{144}Sm and ^{154}Sm , offer an estimated contribution of neutron skin in the isotopic ratio greater than 0.1% and one can expect that a pair of the lightest and the heaviest isotope in Fr or Ra would produce even greater neutron skin contribution.

VI. CONCLUSION

In this work, we provided numerical evaluation of the dependence of spin-independent PNC effect on new physics and neutron skin effects for atoms of current experimental interest. On the basis of the data presented above, one can select the most suitable isotopes and pairs of isotopes for further PNC experiments. We estimated the size of neutron skin corrections for both single isotopes and isotopic ratios. If a 0.1% accuracy in the isotopic ratio measurement is reached, neutron skin effects can be detected in any of the eight elements presented in Table II, given that isotopes with the largest difference in neutron number ΔN are chosen. It was discovered that the uncertainty in Fermi-model diffuseness z (and, therefore, in the model of nuclear density in general) plays a crucial role in the extraction of the neutron skin from the single-isotope experiments, which poses a challenge for improvement of nuclear models.

Isotopic ratios give an opportunity to probe new physics corrections to the standard model proton couplings in low-energy experiments, and, in contrast to single-isotope experiments, without the need to calculate many-body electronic factor of the PNC amplitude. If the neutron skin uncertainties cancel out [29], isotopic ratios can constitute a valuable tool for the search of a list of new physics scenarios, such as new Z' bosons [1, 2, 22, 23]. We found that if a large contribution of neutron skin is to be avoided, it may be beneficial to choose a pair of isotopes with a large ΔN of one of the lighter elements. On the other hand, for experiments aiming at detecting the neutron skin, heavier elements

such as Yb, Pb, Fr and Ra possess a pronounced neutron skin contribution to the PNC effects.

VII. ACKNOWLEDGEMENTS

This work is supported by the Gutenberg Research College fellowship and Australian Research Council. The authors would like to thank Pierre Capel, Sonia Bacca and Vladimir Zelevinsky for valuable discussions.

Appendix

To obtain the radial dependence of one-electron s and $p_{1/2}$ wave functions, we assume the nucleus to be a sharp-edge charged sphere with radius R_p . In this approximation, the electron experiences the potential of a 3D harmonic oscillator inside the nucleus:

$$V(r) = \frac{-Ze^2}{R_p} \left(\frac{3}{2} - \frac{r^2}{2R_p^2} \right). \quad (61)$$

Thus, wave functions inside the nucleus are those of a quantum relativistic harmonic oscillator. Outside the nucleus, they should be relativistic Coulomb wave functions of a point charge. The harmonic-oscillator wave functions should be properly normalized to match Coulomb wave functions (presented, for example, in [30]) at the edge of the nucleus. The s and $p_{1/2}$ wave functions inside the nucleus can be thus written as [30, 31]:

$$\psi_{s_{1/2}} = \begin{pmatrix} F_s \Omega_s \\ iG_s \Omega_{p_{1/2}} \end{pmatrix}, \quad (62)$$

$$\psi_{p_{1/2}} = \begin{pmatrix} -\frac{A_p}{A_s} G_s \Omega_{p_{1/2}} \\ i\frac{A_p}{A_s} F_s \Omega_s \end{pmatrix}, \quad (63)$$

where Ω_s and $\Omega_{p_{1/2}}$ are spherical functions with spin (eigenfunctions of total angular momentum operators \hat{J}_z and \hat{J}^2), normalized as $\int d\phi \int d\theta \Omega^\dagger \Omega = 1$. Denoting $x = r/R_p$, one can write a Taylor expansion of the oscillator radial functions inside the nucleus up to $Z^2\alpha^2$ order [30, 31]:

$$F_s(x) = A_s \left[1 - \frac{3}{8} Z^2 \alpha^2 x^2 \left(1 - \frac{4}{15} x^2 + \frac{1}{45} x^4 \right) \right], \quad (64)$$

$$G_s(x) = -\frac{1}{2} A_s Z \alpha x \times \left[1 - \frac{1}{5} x^2 - \frac{9}{40} Z^2 \alpha^2 x^2 \left(1 - \frac{3}{7} x^2 + \frac{4}{81} x^4 \right) \right]. \quad (65)$$

Here the normalization constants A_s and A_p can be approximated [30] as

$$A_s = \frac{2}{(z_i + 1)^{1/2}} \frac{2(\frac{a_B}{2ZR_p})^{1-\gamma}}{\Gamma(2\gamma + 1)} \left(\frac{Z}{a_B^3}\right)^{1/2} \times \left(\frac{I}{Ry}\right)^{3/4} \left(1 - \frac{1}{40}Z^2\alpha^2\right), \quad (66)$$

$$A_p = \frac{Z\alpha}{(z_i + 1)^{1/2}} \frac{2(\frac{a_B}{2ZR_p})^{1-\gamma}}{\Gamma(2\gamma + 1)} \left(\frac{Z}{a_B^3}\right)^{1/2} \times \left(\frac{I}{Ry}\right)^{3/4} \left(1 + \frac{9}{40}Z^2\alpha^2\right), \quad (67)$$

with $\gamma = \sqrt{1 - Z^2\alpha^2}$, I being the ionization energy of the valence electron and the Rydberg constant $Ry = e^2/(2a_B)$. The Bohr radius is denoted as a_B .

Let us expand the expression used in calculating the matrix element (12) with the wave functions defined above:

$$\psi_{p_{1/2}}^\dagger \gamma_5 \psi_s = -i \frac{A_p}{A_s} \left(G_s^2 \Omega_{p_{1/2}}^\dagger \Omega_{p_{1/2}} + F_s^2 \Omega_s^\dagger \Omega_s \right) \quad (68)$$

If we denote $f_s = F_s/A_s$ and $g_s = G_s/A_s$ and take into account the normalization of spherical functions, then

$$\begin{aligned} \int \psi_{p_{1/2}}^\dagger \gamma_5 \psi_s d^3r &= -i \frac{A_p}{A_s} \int_0^\infty (G_s^2 + F_s^2) dr \\ &= -i A_p A_s \int_0^\infty (g_s^2 + f_s^2) dr \\ &\equiv \mathcal{A}_{ps} \left(\frac{2ZR_p}{a_B}\right)^{2\gamma-2} \int_0^\infty f_{ps}(r) dr. \end{aligned}$$

Here $f_{ps}(r)$, such that $f_{ps}(0) = 1$, contains the variation of wave functions density inside the nucleus, the normalization coefficient $\mathcal{N} \equiv (2ZR_p/a_B)^{2\gamma-2}$ shows the dependence of the expression on equivalent charge radius and \mathcal{A}_{ps} consists of all remaining constants. We use above definitions to calculate the matrix element (12) in the main text.

-
- [1] M. Safronova, D. Budker, D. DeMille, D. F. J. Kimball, A. Derevianko, and C. W. Clark, *Reviews of Modern Physics* **90**, 025008 (2018).
- [2] D. Antypas, A. Fabricant, J. E. Stalnaker, K. Tsigutkin, V. V. Flambaum, and D. Budker, *Nature Physics* **15**, 120 (2019).
- [3] J. Zhang, R. Collister, K. Shiells, M. Tandecki, S. Aubin, J. A. Behr, E. Gomez, A. Gorelov, G. Gwinner, L. A. Orozco, et al., *Hyperfine Interactions* **237**, 150 (2016).
- [4] S. J. Pollock, E. N. Fortson, and L. Wilets, *Physical Review C* **46**, 2587 (1992).
- [5] V. V. Flambaum and I. B. Khriplovich, *Soviet Physics-JETP* **52**, 835 (1980), [*Sov. Phys. JETP* 52 (1980) 835].
- [6] J. S. M. Ginges and V. V. Flambaum, *Physics Reports* **397**, 63 (2004).
- [7] M. Tanabashi, K. Hagiwara, K. Hikasa, K. Nakamura, Y. Sumino, F. Takahashi, J. Tanaka, K. Agashe, G. Aielli, C. Amisler, et al., *Review of Particle Physics* (Particle Physics Properties PDG RPP, 2018).
- [8] A. Ong, J. C. Berengut, and V. V. Flambaum, *Physical Review C* **82**, 014320 (2010).
- [9] M. J. Ramsey-Musolf, *Physical Review C* **60**, 015501 (1999).
- [10] PREX Collaboration, S. Abrahamyan, Z. Ahmed, H. Albatineh, K. Aniol, D. S. Armstrong, W. Armstrong, T. Averett, B. Babineau, A. Barbieri, et al., *Physical Review Letters* **108**, 112502 (2012).
- [11] C. S. Wood, S. C. Bennett, D. Cho, B. P. Masterson, J. L. Roberts, C. E. Tanner, and C. E. Wieman, *Science* **275**, 1759 (1997).
- [12] V. A. Dzuba, V. V. Flambaum, and J. S. M. Ginges, *Physical Review D* **66**, 076013 (2002).
- [13] S. G. Porsev, K. Beloy, and A. Derevianko, *Physical Review Letters* **102**, 181601 (2009).
- [14] V. A. Dzuba, J. C. Berengut, V. V. Flambaum, and B. Roberts, *Physical Review Letters* **109**, 203003 (2012).
- [15] A. Derevianko, *Physical Review A* **65**, 012106 (2001).
- [16] M. A. Bouchiat and C. Bouchiat, *Journal de Physique* **35**, 899 (1974).
- [17] V. A. Dzuba, V. V. Flambaum, and I. B. Khriplovich, *Zeitschrift für Physik D Atoms, Molecules and Clusters* **1**, 243 (1986).
- [18] E. N. Fortson, Y. Pang, and L. Wilets, *Physical Review Letters* **65**, 2857 (1990).
- [19] A. Derevianko and S. G. Porsev, *Physical Review A* **65**, 052115 (2002).
- [20] L. C. Chamon, B. V. Carlson, L. R. Gasques, D. Pereira, C. De Conti, M. A. G. Alvarez, M. S. Hussein, M. A. Cândido Ribeiro, E. S. Rossi, and C. P. Silva, *Physical Review C* **66**, 014610 (2002).
- [21] J. James and P. G. H. Sandars, *Journal of Physics B: Atomic, Molecular and Optical Physics* **32**, 3295 (1999).
- [22] H. Davoudiasl, H.-S. Lee, and W. J. Marciano, *Physical Review D* **89**, 095006 (2014).
- [23] V. Dzuba, V. Flambaum, and Y. Stadnik, *Physical Review Letters* **119**, 223201 (2017).
- [24] J. Jänecke, *Physics Letters* **103B**, 1 (1981).
- [25] W. H. King, *Isotope Shifts in Atomic Spectra* (Springer Science & Business Media, 2013).
- [26] O. P. Sushkov and V. V. Flambaum, *Sov. Phys. JETP* **48**, 453 (1978), [*Zh. Eksp. Teor. Fiz.* 75, 1208 (1978)].
- [27] V. V. Flambaum, V. A. Dzuba, and C. Harabati, *Physical Review A* **96**, 012516 (2017).
- [28] I. Angeli and K. P. Marinova, *Atomic Data and Nuclear Data Tables* **99**, 69 (2013).
- [29] B. A. Brown, A. Derevianko, and V. V. Flambaum, *Physical Review Letters* **102**, 181601 (2009).

- ical Review C **79**, 035501 (2009).
- [30] I. B. Khriplovich, *Parity nonconservation in atomic phenomena* (Gordon and Breach, 1991), 2nd ed.
- [31] V. V. Flambaum and J. S. M. Ginges, Physical Review A **65**, 032113 (2002).